PCCP

Accepted Manuscript

ROYAL SOCIETY OF CHEMISTRY

www.rsc.org/pccp

First-principles study of electronic structure and mechanical and optical properties of $CaAlSiN_3$

Zhanyu Wang[a], Bo Shen[a], Fei Dong[a], Songyou Wang[a,b#] and Wan-Sheng Su[c*]

[a]*Shanghai Ultra-Precision Optical Manufacturing Engineering Center and Department of Optical Science and Engineering, Fudan University, Shanghai, 200433, China*

[b]*Key Laboratory for Information Science of Electromagnetic Waves (MoE), Shanghai 200433, China*

[c]*National Center for High-Performance Computing, Hsinchu 30076, Taiwan and Department of Physics, National Chung Hsing University, Taichung 40227, Taiwan*

E-mail: songyouwang@fudan.edu.cn (S Wang) and wssu@nchc.narl.org.tw (W. S. Su)

Abstract

The mechanical properties, electronic structures and optical properties of $CaAlSiN_3$ were investigated using the first-principles calculations. The elastic constants, bulk moduli, shear moduli, Young's moduli, and Poisson's ratio were obtained. These results indicate $CaAlSiN_3$ is mechanically stable and a relatively hard material. Moreover, this compound has an indirect band gap of ~ 3.4 eV according to its band structure and density of states. The linear photon energy dependent dielectric functions and related optical properties including refractive index, extinction coefficient, absorption spectrum, reflectivity, and energy loss spectrum were computed and discussed. It is shown that no sizable anisotropy is found in the optical properties of $CaAlSiN_3$. The obtained structural estimation and some other results are in agreement with available experimental and theoretical data. This investigation is not only helpful for better understanding the electronic, mechanical and optical properties of $CaAlSiN_3$, but also will open the possibility of its use in device applications.

Keywords: Structural properties, Elastic constants, Electronic properties, Optical properties

Introduction

Multinary silicon-nitride based materials have been explored extensively and developed for use in white light emitting diode (LED) devices when doped with rare-earth ions (typically Eu^{2+} or Ce^{3+}). This is due to their many advantages, including adequate thermal and environmental stability, excellent thermal quenching characteristics, and high luminescence efficiency under excitation at near-ultraviolet to blue light from an InGaN diode.[1-5] Among the reported phosphors for LED applications, $CaAlSiN_3:Eu^{2+}$, which exhibits efficient red luminescence excited by blue light, is one of the most promising for practical applications.[6-14] As the host material, $CaAlSiN_3$, has an orthorhombic structure and crystallizes in the $Cmc2_1$ space group.[10] There are four formula units per unit cell, with Al and Si atoms randomly distributed among the same tetrahedral sites coordinated by four nitrogen atoms, as illustrated in Fig. 1.[15] All AlN_4/SiN_4 tetrahedra form six-membered rings by sharing the corner, and the rings are combined to constitute the planes. In addition, Ca atoms coordinated to five N atoms are accommodated in cavities in the overlaid planes.

Several experimental and theoretical studies of $CaAlSiN_3$ have been carried out. For example, Huang *et al.*[16] synthesized $CaAlSiN_3$ in a $CaO–Si_3N_4–AlN$ system and measured the lattice parameters. In 2004, $CaAlSiN_3$ was prepared by reaction of silicon diimide $[Si(NH)_2]$ with corresponding metals, and single crystal diffraction structure analysis was then performed to investigate the crystal structure.[17] Subsequently, Uheda *et al.*[18] confirmed the orthorhombic structure of $CaAlSiN_3$ by convergent beam electron diffraction. In addition, the atomic and electronic structure of $CaAlSiN_3$ has also been explored by first-principles method.[15] Since Uheda[11] reported the luminescence properties of $CaAlSiN_3:Eu^{2+}$ red phosphor, extensive research has been performed in recent years on $CaAlSiN_3$ doped with rare-earth ions as well as its isostructural (oxy) nitrides. In order to take full advantage of the properties of $CaAlSiN_3$ for eventual technological applications, a better understanding of its electronic structure, mechanical and optical properties is required. However, to

the best of our knowledge, understanding of a number of basic characteristics of this compound is still far from complete.

In this work, we present a systematic study of $CaAlSiN_3$ by means of first-principles calculations. The computational models are constructed by assuming the order of Al/Si distributions in the primitive unit cell. The paper is organized as follows: in Section 2, the computational techniques adopted in this study are described in detail. Results and discussion of the electronic, structural, mechanical and optical properties are presented in Section 3. Finally, conclusions are given in Section 4.

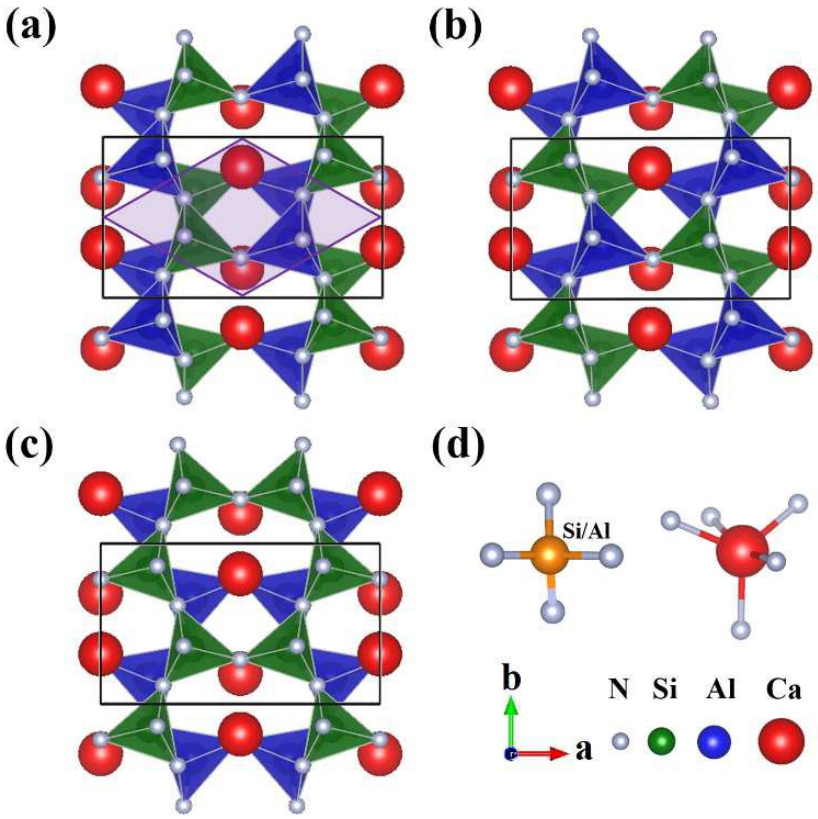

Fig. 1. (Color online) Projective representation of the crystal structure for (a) Phase-I, (b) Phase-II, and (c) Phase-III of orthorhombic $CaAlSiN_3$ crystal illustrated with AlN_4/SiN_4 tetrahedra. The primitive unit cell is highlighted by a parallelogram in (a). (d) The coordination environment of Al/Si and Ca atoms.

Computational details

The static lattice energy and the Hellmann-Feynman force calculations were carried out using the density functional theory (DFT), implemented in the Vienna *ab initio* simulation package (VASP).[19-21] The projector-augmented wave function (PAW) method[22] with generalized gradient approximation (GGA) was applied, with the Perdew-Burke-Ernzerh [23] (PBE) of exchange correlation functional. The plane-wave energy cutoff was 520 eV. The Brillouin zone was sampled by a 7×9×9 Monkhorst-Pack[24] k mesh. The total energy was calculated with high precision, and converged to 10^{-6} eV/atom. The lattice constants and the atom coordinates were optimized until the interatomic forces were less than 10^{-2} eV/Å.

The unit cell of the $CaAlSiN_3$ crystal containing 24 atoms was utilized as the computational model. Placing two Al atoms and two Si atoms in the four tetrahedral sites of the primitive cell gives six such Al/Si-ordered phases. However, when the crystal symmetry is considered, only three patterns among them, depicted in Fig. 1(a-c), are obtained. In terms of the chemical properties, the other three phases are equivalent to the present ones, respectively.[15]

The popular 'stress–strain' method[25] for determining the elastic constants implemented in VASP is used in this study. The traditional mechanical stability conditions in orthorhombic crystals at equilibrium are expressed in terms of elastic constants as follows:[26]

$$\begin{aligned} &C_{11}>0,\ C_{22}>0,\ C_{33}>0,\ C_{44}>0,\ C_{55}>0,\ C_{66}>0,\\ &C_{11}+C_{22}+C_{33}+2\left(C_{12}+C_{13}+C_{23}\right)>0,\\ &\left(C_{11}+C_{22}-2C_{12}\right)>0,\ \left(C_{11}+C_{33}-2C_{13}\right)>0,\ \left(C_{22}+C_{33}-2C_{23}\right)>0. \end{aligned} \quad (1)$$

The bulk moduli B and shear moduli G are calculated in terms of elastic constants using the following relations [26]

$$B_V=(1/9)\left[C_{11}+C_{22}+C_{33}+2\left(C_{12}+C_{13}+C_{23}\right)\right],$$

$$G_V=(1/15)\left[C_{11}+C_{22}+C_{33}+3\left(C_{44}+C_{55}+C_{66}\right)-\left(C_{12}+C_{13}+C_{23}\right)\right],$$

$$B_R = \Delta\left[C_{11}\left(C_{22}+C_{33}-2C_{23}\right)+C_{22}\left(C_{33}-2C_{13}\right)-2C_{33}C_{12}\right.$$
$$\left.+C_{12}\left(2C_{23}-C_{12}\right)+C_{13}\left(2C_{12}-C_{13}\right)+C_{23}\left(2C_{13}-C_{23}\right)\right]^{-1},$$

$$G_R = 15\left\{4\left[C_{11}\left(C_{22}+C_{33}+C_{23}\right)+C_{22}\left(C_{33}+C_{13}\right)+C_{33}C_{12}\right.\right.$$
$$\left.-C_{12}\left(C_{23}+C_{12}\right)-C_{13}\left(C_{12}+C_{13}\right)-C_{23}\left(2C_{13}+C_{23}\right)\right]/\Delta,$$
$$\left.+3\left[\left(1/C_{44}\right)+\left(1/C_{55}\right)+\left(1/C_{66}\right)\right]\right\}^{-1}$$

$$\Delta = C_{13}\left(C_{12}C_{23}-C_{13}C_{22}\right)+C_{23}\left(C_{12}C_{13}-C_{23}C_{11}\right)+C_{33}\left(C_{11}C_{22}-C_{12}^2\right), \quad (2)$$

where the subscripts V and R indicate the Voigt and Reuss bound, respectively. It is known that the Voigt bound is the upper limit of the actual effective moduli, while the Reuss bound is the lower limit. The arithmetic average of Voigt and Reuss bounds is termed as the Voigt-Reuss-Hill approximation[27],

$$M_H = \left(1/2\right)\left(M_R + M_V\right),\ M_H = B_H,\ G_H. \quad (3)$$

Young's moduli Y and Possion ratio ν can be given by

$$Y = 9BG/\left(3B+G\right),\ \nu = \left(3B-2G\right)/\left[2\left(3B+G\right)\right]. \quad (4)$$

The corresponding optical properties are determined by the complex dielectric function $\varepsilon(\omega)$ which can be calculated by the so-called independent particle approximation as implemented in VASP.[28] The quasiparticle self-energy corrections, local-field effects, and excitonic contributions are neglected in our calculations.[29] The imaginary part of the dielectric function is obtained from the momentum matrix elements between the occupied and unoccupied wave functions within the selection rules and given by[30, 31]

$$\varepsilon_2\left(\omega\right) = \frac{2e^2\pi}{\Omega\varepsilon_0}\sum_{k,v,c}\left|\left\langle\psi_k^c\left|\hat{u}\times r\right|\psi_k^v\right\rangle\right|^2\delta\left(E_k^c - E_k^v - E\right), \quad (5)$$

where Ω is the unit-cell volume, ψ_k^c and ψ_k^v are the conduction band and valence band wave functions at k, respectively. The real part of dielectric function follows from the Kramer–Kronig relationship.[32] Furthermore, all other optical constants on the energy dependence of refractive index, extinction coefficient, absorption spectrum,

reflectivity, and energy loss spectrum can be derived from $\varepsilon_1(\omega)$ and $\varepsilon_2(\omega)$.

Results and discussion

Structure

Fig. 1 shows the three possible atomic configurations for the unit cell of the $CaAlSiN_3$ crystal. After geometric optimization, the attained structures are very close to the experimental orthorhombic structure[17, 18]. Additionally, the calculated structural data are almost the same as the available theoretical data reported by Mikami *et al*[15]. The lattice constants *a*, *b* and *c* are 9.917 Å, 5.691 Å and 5.075 Å for phase-I, 9.915 Å, 5.690 Å and 5.076 Å for phase-II, and 9.878 Å, 5.648 Å and 5.127 Å for phase-III. It shows that phase-I and phase-II have nearly the same lattice parameters, and their lattice constants *a* and *b* are slightly larger than that of phase-III, whereas their lattice constants *c* are slightly smaller than that of phase-III. These predicted lattice constants agree well with the corresponding experimental values; however, these discrepancies might be related to the fact that the GGA calculations overestimate the lattice constants slightly.

The cohesive energy of $CaAlSiN_3$ crystal is defined as $E_c = E_{\text{total}} - 4\times\left(E_{\text{Ca atom}} + E_{\text{Al atom}} + E_{\text{Si atom}} + 3\times E_{\text{N atom}}\right)$, where E_{total} is the total energy of $CaAlSiN_3$ unit cell, and $E_{\text{Ca atom}}$, $E_{\text{Al atom}}$, $E_{\text{Si atom}}$ and $E_{\text{N atom}}$ are the energies of the corresponding isolated atoms. The calculations show that the cohesive energies of phase-I, phase-II and phase-III are -5.5781 eV, -5.5778 eV and -5.5484 eV, respectively. It can be seen that the negative cohesive energies follow the order of phase-I < phase-II < phase-III, but the values of phase-I and phase-II are very close. Note that when the value of cohesive energy becomes more negative, the corresponding $CaAlSiN_3$ structure becomes more favorable.

The formation energy of the $CaAlSiN_3$ unit cell, defined as $E_f = E_{total} - 4\times\left(E_{\text{Ca}}^{bulk} + E_{\text{Al}}^{bulk} + E_{\text{Si}}^{bulk} + 3\times E_{\text{N}}^{dimer}\right)$, is also demonstrated. Here,

E_{Ca}^{bulk} and E_{Al}^{bulk} represent the atomic energies in face-centered cubic structures, E_{Si}^{bulk} in a diamond structure, and E_{N}^{dimer} in a molecular dimer. The calculated formation energy E_f of phase-I, phase-II and phase-III are -5.5781 eV, -5.5778 eV and -5.5484 eV, respectively. All the studied phases have negative formation energies, which manifest the structural stability of these phases. Further, this indicates that their composition processes from elemental forms are exothermic reactions. Comparing E_c and E_f of $CaAlSiN_3$, it is clear that phase-III has slightly higher cohesive and formation energies than the other two phases. Furthermore, due to the similarity in lattice parameters as well as the cohesive and formation energies of the phase-I and phase-II unit cells, the $CaAlSiN_3$ compound may prefer to crystallize in a mixing structure which is composed of those two phases. This result appears consistent with previous observations based on Pauling's second crystal rule[15].

Mechanical properties

The elastic properties, including elastic constants, bulk moduli, shear moduli, Young's moduli and Poisson's ratio, give corresponding information about the response of mechanical stability, stiffness and mechanical nature of materials to applied stress. For the orthorhombic $CaAlSiN_3$ crystal, the values of nine independent elastic constants are tabulated in Table 1. It can be seen that the criteria described by Eq. 1 are satisfied, which indicate these three phases of $CaAlSiN_3$ are structural and mechanically stable.

Table 1. Calculated elastic constants (C_{ij} in GPa) for orthorhombic $CaAlSiN_3$ crystal.

Structural	C_{11}	C_{22}	C_{33}	C_{44}	C_{55}	C_{66}	C_{12}	C_{13}	C_{23}
Phase -I	328.9	285.9	323.3	67.0	110.7	83.1	116.3	69.2	99.9
Phase -II	324.1	287.0	322.0	68.6	110.2	84.4	117.7	71.9	98.1
Phase -III	329.3	288.3	315.3	69.4	104.5	81.7	116.6	73.6	95.2

Through Eqs. 2 and 3, the macroscopic mechanical properties of the $CaAlSiN_3$ crystal, namely bulk moduli, shear moduli, Young's moduli, and Poisson's ratio, can

be determined by the obtained elastic constants. The attained results are summarized in Table 2. We can see from this table that the differences among the bulk moduli of the three phases as well as the shear moduli are comparatively small, and all the bulk moduli for three phases are large. A comparison with bulk moduli of 103(5) GPa for $SrSi_2O_2N_2$:Eu, which shows valuable luminescence properties[33], suggests that $CaAlSiN_3$ might be a relatively hard material. In addition, we can see that B_H is larger than G_H, which implies that the shear moduli G_H limits the stability of these phases. Furthermore, the calculated values of the Poisson's ratio for three phases in PBE are ~ 0.27.

Table 2. Calculated bulk moduli (B_V, B_R, B_H, in GPa), shear moduli (G_V, G_R, G_H, in GPa), Young's moduli (Y, in GPa), and Poisson's ratio (ν) for orthorhombic $CaAlSiN_3$ crystal.

Structural	B_V	B_R	B_H	G_V	G_R	G_H	Y	ν
Phase -I	167.7	167.5	167.6	95.7	87.1	91.4	232.0	0.27
Phase -II	167.6	167.5	167.5	95.7	87.5	91.6	232.4	0.27
Phase -III	167.1	166.8	166.9	94.3	86.8	90.5	230.0	0.27

Electronic properties

In order to analyze the electronic properties of the $CaAlSiN_3$ crystal, the energy band structures and the density of states (DOSs) for the three phases are illustrated in Figs. 2 and 3, respectively. The valence band maximum is set to 0 eV in each case. The main features of the band structures and the DOS plots appear similar. Since the optical spectra are captured from interband transitions, which are those taking place between valence and conduction bands which are in turn relative to the band gap, it is necessary to measure the magnitude of the band gap. From Fig. 2, it is observed that the bottom of the conduction band occurs at the Γ point. The top branches of the valence bands for the three phases are very flat. Their maximums are at 0.38 from Γ to Z for phase-I and phase-II, and 0.1 from Γ to Z for phase-III. Hence, our PBE calculations indicate that phase-I and phase-II have an indirect band gap of 3.36 eV, and phase-III has an indirect band gap of 3.4 eV. The magnitude of the calculated gap

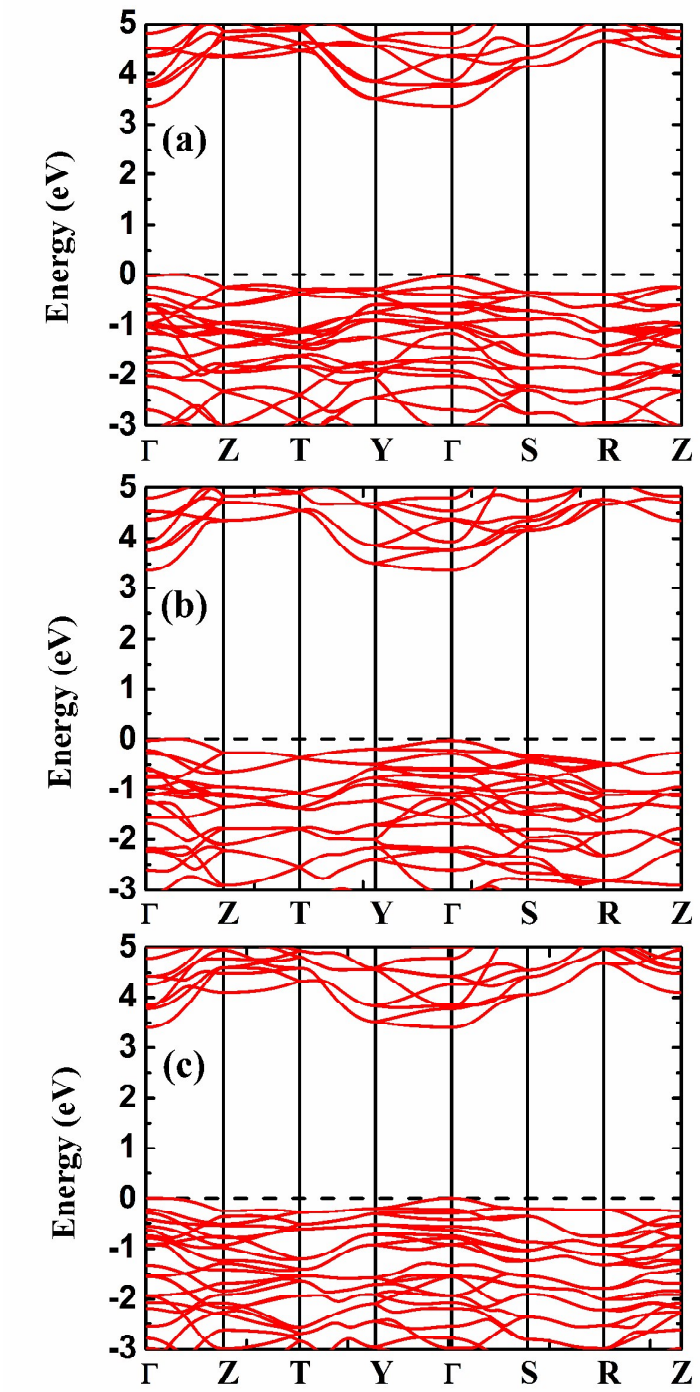

Fig. 2. Calculated band structures of (a) phase-I, (b) phase-II, and (c) phase-III of the $CaAlSiN_3$ crystal, along with the high-symmetry points of the Brillouin zone.

agrees quite well with other reported theoretical data[15]. As expected, our calculated gap is smaller than the experimentally reported value [34] of 3.82 eV owing to the

underestimation of band gap in such a DFT scheme. The band structure of phase-II was also calculated using hybrid exchange-correlation functional (HSE06)[35]. However, HSE06 greatly overestimates the band-gap of phase-II with a value of 4.76 eV. Accordingly, the electronic properties and optical properties of $CaAlSiN_3$ were calculated using standard DFT.

As can be seen from the total and partial density of states for the three phases presented in Fig. 3, the conduction bands are composed mostly of Ca 3d states which show a hybridization character with Al/Si 3s/3p states. The energy bands between about −7.5 and 0 eV are dominated by hybridizing Ca 3d, Al/Si 3s/3p and N 2p states, and the top of the valence bands reflect the p electronic character. The lower valence bands are attributed to Al/Si 3s/3p and N 2s states.

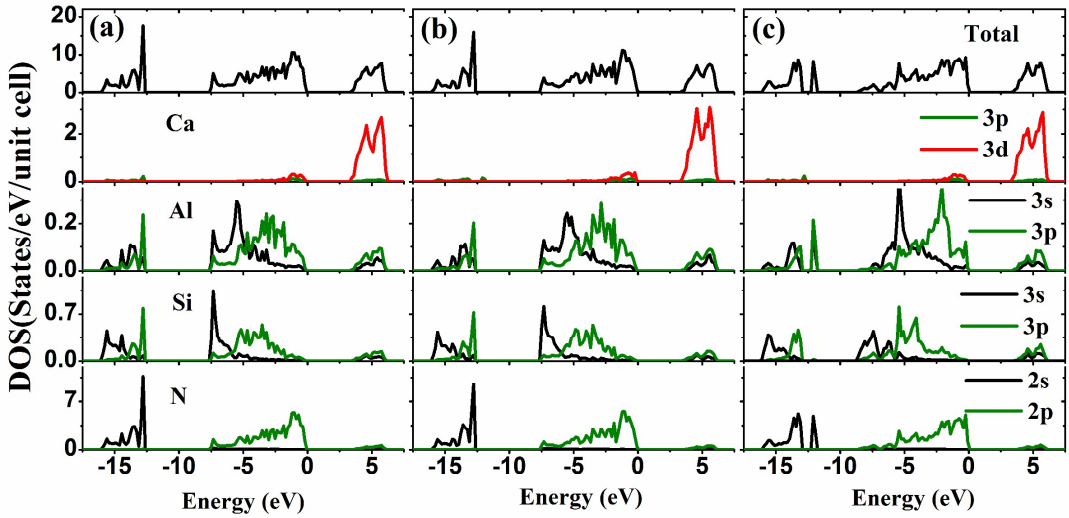

Fig. 3. Calculated partial and total densities of states diagrams for (a) phase-I, (b) phase-II, and (c) phase-III of the $CaAlSiN_3$ crystal. All the states are shown using the same graph legend. Ca 3s states are mainly located at much lower valence bands and are not shown in the figure.

Optical properties

Here, optical properties of $CaAlSiN_3$ crystal are calculated and discussed. Due to the orthorhombic structure, the single crystal of $CaAlSiN_3$ is optically a biaxial system. For such a reason, its linear dielectric tensor has three independent components that

are the diagonal elements of the dielectric tensor. Fig. 4 displays the imaginary $\varepsilon_2(\omega)$ and real $\varepsilon_1(\omega)$ parts of the dielectric functions as a function of the photon energy for the three phases. It is clearly seen that the behavior of the three independent components of $\varepsilon(\omega)$ are very similar; that is, the optical properties of orthorhombic $CaAlSiN_3$ show no sizable anisotropy. The absorption occurs at ~ 3.4 eV, which is clearly nearly equal to the band gap. The overall shape of the $\varepsilon_2(\omega)$ line, characterized by two distinct broad peaks below and above ~22 eV, is very complex. As observed in the figure, these two main peaks for phase-II of polarization direction (010) exhibit triplet structures.

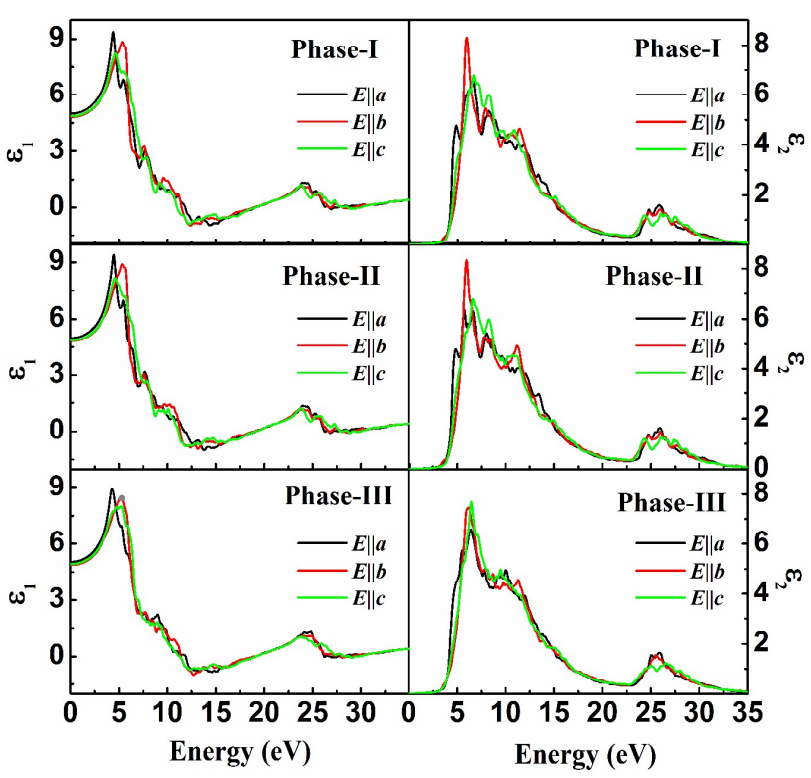

Fig. 4. Calculated imaginary $\varepsilon_2(\omega)$ and real $\varepsilon_1(\omega)$ parts of the dielectric function versus photon energy of the $CaAlSiN_3$ crystal for different light polarizations.

The origins of the different peaks in the calculated $\varepsilon_2(\omega)$ can be attributed to interband transitions. According to selection rules, only the transitions which imply a change of the angular momentum quantum number l by 1 are allowed. For example,

the first triplet structure (especially the maximum peak ~ 6 eV) for $E||b$ of phase-II can be mainly assigned to transitions from N 2p to Ca 3d states. Transitions from Al/Si 3p to Ca 3d also give rise to the peak ~ 8 eV. The contributions from transitions from Al/Si 3s to Al/Si 3p are also very large for the peak ~ 11 eV. Moreover, the second triplet structure (~ 22 eV) is mainly due to the transition from the Al/Si 3s, Al/Si 3p and N 2s states, which correspond to the lower valence bands between −15.9 and −12.8 eV to the conduction bands. Note that a peak in $\varepsilon_2(\omega)$ does not correspond to a single interband transition since many direct or indirect transitions may be found in a band structure with an energy corresponding to the same peak.

For the $E||b$ of phase-II, the calculated static dielectric constant $\varepsilon_1(0)$ was found to be 4.82. The $\varepsilon_1(\omega)$ becomes negative at 11.3 eV and then a positive return occurs at 19 eV. Fig. 5(a)–(d) depicts the calculated results of refractive index and extinction coefficient, absorption spectrum, reflectivity, and energy loss spectrum, respectively, for the $E||b$ of phase-II. The static refractive index is found to have a value of 2.19. The refractive index reaches a maximum value of 3.12 at 5.71 eV. There is no absorption and only a small reflectivity in the photon-energy range up to 3.3 eV, meaning that the material becomes transparent in this region. The energy-loss spectrum describes the energy loss of a fast electron traversing a material. The main peak is located at ~ 30.9 eV, which is generally defined as the bulk plasma frequency, corresponding to the trailing edges in the reflection spectra. Since there is no sizable anisotropy displayed in the optical properties of orthorhombic $CaAlSiN_3$, the optical properties of the three phases for different light polarizations are similar to those for the phase-II of polarization direction (010).

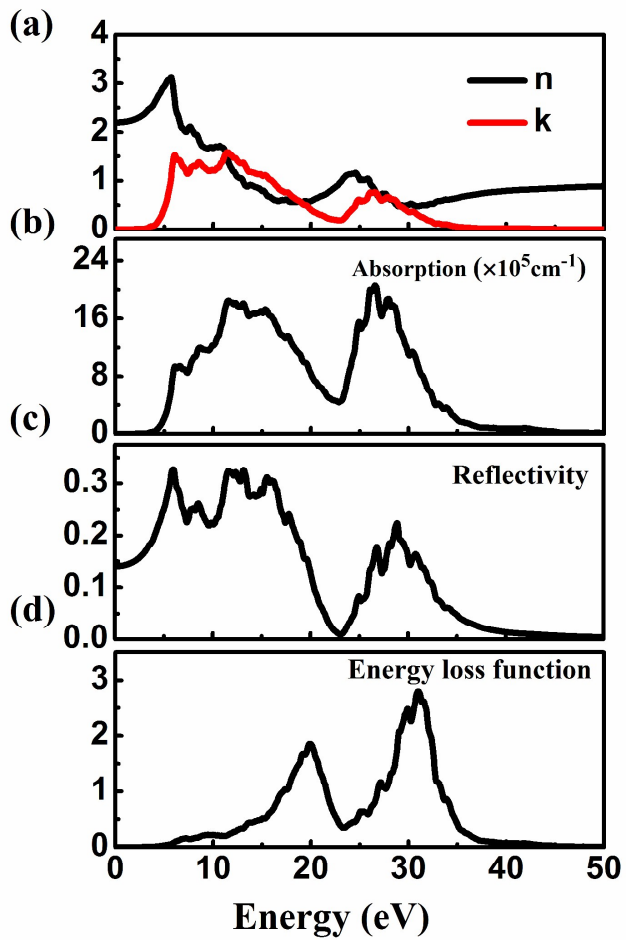

Fig. 5. Calculated optical constants for E||b of phase-II $CaAlSiN_3$: (a) refractive index n and extinction coefficient k, (b) absorption spectrum, (c) reflectivity, and (d) energy-loss spectrum.

Conclusions

In summary, first principles calculations have been performed to obtain the structural, electronic, elastic and optical properties of the orthorhombic $CaAlSiN_3$ compound. The crystal structure has been built by distributing the Al/Si atoms in order in the primitive unit cell. Phase-I and phase-II were found to have slightly lower cohesive and formation energies than phase-III. Our attained structural parameters are in agreement with the experimental data. The calculated elastic constants meet traditional mechanical stability conditions, demonstrating that $CaAlSiN_3$ is mechanically stable. The other mechanical data including bulk moduli, shear moduli, Young's moduli, and Poisson's ratio are also determined. The electronic structure

demonstrates that $CaAlSiN_3$ has an indirect band gap of ~ 3.4 eV. The magnitude of the calculated gap agrees quite well with other reported theoretical data, and is slightly smaller than the experimentally reported value of 3.82 eV. Finally, the complex dielectric function has been shown, and the three independent components of $\varepsilon(\omega)$ reveal that the optical properties of orthorhombic $CaAlSiN_3$ show no sizable anisotropy. For phase-II of the polarization direction (010), the dielectric function, refractive index, extinction coefficient, absorption spectrum, reflectivity, and energy loss spectrum were obtained and discussed. Our investigations are helpful not only for the understanding the electronic, mechanical and optical properties of $CaAlSiN_3$ but also open the possibility of its use in device applications.

Acknowledgements

W. S. Su would like to thank the National Science Council of Taiwan for financially supporting this research under Contract No. NSC-101-2112-M-492-001-MY3. Support from the National Centers for Theoretical Sciences (South) and High-performance Computing of Taiwan in providing huge computing resources to facilitate this research are also gratefully acknowledged. The work at Fudan University was supported by the National Natural Science Foundation of China (Grant Nos. 11374055 and 10974029), the National Basic Research Program of China (Nos. 2010CB933703 and 2012CB934303), and the Fudan High-end Computing Center.

References

[1] R.-J. Xie, H. T. Bert Hintzen, and D. Johnson, Journal of the American Ceramic Society **96**, 665 (2013).

[2] R. J. Xie, N. Hirosaki, K. Sakuma, Y. Yamamoto, and M. Mitomo, Applied Physics Letters **84**, 5404 (2004).

[3] C. J. Duan, X. J. Wang, W. M. Otten, A. C. A. Delsing, J. T. Zhao, and H. T. Hintzen, Chemistry of Materials **20**, 1597 (2008).

[4] Y. Q. Li, G. de With, and H. T. Hintzen, Journal of Luminescence **116**, 107 (2006).

[5] R. J. Xie, N. Hirosaki, M. Mitomo, Y. Yamamoto, T. Suehiro, and K. Sakuma, Journal of Physical Chemistry B **108**, 12027 (2004).

[6] Y. Q. Li, N. Hirosaki, R. J. Xie, T. Takeda, and M. Mitomo, Chemistry of Materials **20**, 6704 (2008).
[7] H. Watanabe, H. Yamane, and N. Kijima, Journal of Solid State Chemistry **181**, 1848 (2008).
[8] J. Yang, T. Wang, D. Chen, G. Chen, and Q. Liu, Materials Science and Engineering: B **177**, 1596 (2012).
[9] B. Lei, K.-i. Machida, T. Horikawa, and H. Hanzawa, Chemistry Letters **39**, 104 (2010).
[10] Z. Zhang, O. M. ten Kate, A. Delsing, E. van der Kolk, P. H. L. Notten, P. Dorenbos, J. Zhao, and H. T. Hintzen, Journal of Materials Chemistry **22**, 9813 (2012).
[11] K. Uheda, N. Hirosaki, Y. Yamamoto, A. Naito, T. Nakajima, and H. Yamamoto, Electrochemical and Solid-State Letters **9**, H22 (2006).
[12] X. Piao, K.-i. Machida, T. Horikawa, H. Hanzawa, Y. Shimomura, and N. Kijima, Chemistry of Materials **19**, 4592 (2007).
[13] J. Li, T. Watanabe, N. Sakamoto, H. Wada, T. Setoyama, and M. Yoshimura, Chemistry of Materials **20**, 2095 (2008).
[14] Y. Q. Li, N. Hirosaki, R. J. Xie, T. Takeda, and M. Mitomo, Chemistry of Materials **20**, 6704 (2008).
[15] M. Mikami, K. Uheda, and N. Kijima, physica status solidi (a) **203**, 2705 (2006).
[16] Z. K. Huang, W. Y. Sun, and D. S. Yan, Journal of Materials Science Letters **4**, 255 (1985).
[17] F. Ottinger, Ph.D, Universität Karlsruhe, 2004.
[18] K. Uheda, H. Yamamoto, H. Yamane, W. Inami, K. Tsuda, Y. Yamamoto, and N. Hirosaki, Journal of the Ceramic Society of Japan **117**, 94 (2009).
[19] G. Kresse and J. Furthmüller, Computational Materials Science **6**, 15 (1996).
[20] G. Kresse and J. Furthmüller, Physical Review B **54**, 11169 (1996).
[21] G. Kresse and D. Joubert, Physical Review B **59**, 1758 (1999).
[22] P. E. Blöchl, Physical Review B **50**, 17953 (1994).
[23] J. P. Perdew, K. Burke, and M. Ernzerhof, Physical Review Letters **77**, 3865 (1996).
[24] H. J. Monkhorst and J. D. Pack, Physical Review B **13**, 5188 (1976).
[25] Y. Le Page and P. Saxe, Phys. Rev. B **65**, 104104 (2002).
[26] Z.-j. Wu, E.-j. Zhao, H.-p. Xiang, X.-f. Hao, X.-j. Liu, and J. Meng, Physical Review B **76** (2007).
[27] R. Hill, Proceedings of the Physical Society. Section A **65**, 349 (1952).
[28] B. Adolph, J. Furthmüller, and F. Bechstedt, Physical Review B **63** (2001).
[29] R. J. Bondi, S. Lee, and G. S. Hwang, Physical Review B **81** (2010).
[30] Q.-J. Liu, Z.-T. Liu, L.-P. Feng, and H. Tian, Solid State Sciences **12**, 1748 (2010).
[31] R. Saniz, L.-H. Ye, T. Shishidou, and A. Freeman, Physical Review B **74** (2006).
[32] B. Holm, R. Ahuja, Y. Yourdshahyan, B. Johansson, and B. Lundqvist, Physical Review B **59**, 12777 (1999).

[33] O. Ermakova, et al., J. Chem. Phys. **141**, 014705 (2014).
[34] K. Takahashi, N. Hirosaki, R.-J. Xie, M. Harada, K.-I. Yoshimura, and Y. Tomomura, Applied Physics Letters **91** (2007).
[35] J. Heyd, G. E. Scuseria, and M. Ernzerhof, Journal of Chemical Physics **124**, 219906 (2006).